



DEVELOPMENT AND EVALUATION OF CURCUMIN-EUDRAGIT MICRO MICROSPONGES FOR ANTI-INFLAMMATORY THERAPY OF COLON

Syed Mohasin Abbas and Preethi Sudheer*

Department of Pharmaceutics, Krupanidhi College of Pharmacy, Bengaluru 560035, India

This study aimed to develop curcumin microsponges to combat colonic inflammation. Curcumin has traditionally been recognized for its anti-inflammatory properties. However, their therapeutic potential is hindered by factors, such as low bioavailability, poor solubility in water, and instability in acidic and neutral environments. Additionally, its limited absorption from the intestine, hepatic metabolism, and rapid elimination limits its effectiveness. To address these issues, this study aimed to improve the solubility of curcumin by creating inclusion complexes with cyclodextrin. These complexes can enhance the therapeutic efficacy, reduce the required dosage, and facilitate drug loading into microsponges. This study commenced with the creation of curcumin inclusion complexes with cyclodextrin, which were assessed for their drug content, solubility, in vitro release, and structural characteristics. Additionally, microsponges of cyclodextrin were developed using a pH-sensitive polymers (Eudragit L100 and S 100) and a pore former (PVA), guided by experimental design (Design Expert version 13) to optimize drug loading and release. The resulting formulations were subjected to FTIR, SEM, and anti-inflammatory activity evaluations using an acetic acid-induced rat colitis model. The inclusion complexes at a 1:1.5 ratio exhibited desirable characteristics, and the optimized microsponges demonstrated a three-fold increase in the drug release rate compared to the pure drug. The anti-inflammatory effect observed in the colon, as evidenced by the recovery of normal morphology after oral administration of the microsponges, indicated the potential of the optimized formulation for targeted drug delivery. In conclusion, curcumin microsponges developed using the eudragit combination showed anti-inflammatory effects on colonic tissues.

Keywords: *curcumin, microsponges, colon targeted, Eudragit*

INTRODUCTION

For a drug delivery system to effectively succeed in pharmacotherapy, the unaltered drug must reach its intended target site or receptor at concentrations exceeding the minimum practical level. Various factors necessitate the precise targeting of a drug to a specific site, including instability, low solubility, short half-life, large volume of distribution, poor absorption, low specificity, and a narrow therapeutic index. Although the colon might not be the optimal location for drug absorption because of the absence of well-defined villi, as seen in the small intestine, it compensates for prolonged contact with the mucosa despite a much smaller surface area¹⁻².

Colon-specific drug delivery systems (DDSs) offer distinct advantages, including

near-neutral pH, extended transit time, reduced enzymatic activity, and elevated local drug concentrations with minimal side effects, which are especially beneficial for anti-inflammatory drugs. These systems also contribute to avoiding undesired digestion and enhancing the bioavailability³⁻⁵.

Multi-particulate strategies involve formulations comprising microscopic particles such as pellets, granules, beads, microparticles, and nanoparticles. These approaches provide benefits, such as enhanced bioavailability, decreased chances of systemic toxicity, lower risk of local irritation, predictable gastric emptying, prolonged retention in the ascending colon, and ease of gastrointestinal transit⁶⁻⁷.

Microsponges are porous, polymeric, microporous, bead-like structures with consistent voids and particle sizes arranged

from 5-300 μ m. Microsponges are specifically designed to efficiently deliver pharmaceutically active ingredients at minimal doses, improve stability, diminish side effects, and alter drug release profiles⁸⁻⁹.

Curcumin, extracted from the *Curcuma longa* turmeric plant, is a naturally occurring herbal polyphenol with an extensive history of usage. It is renowned for its varied effects, including its anti-inflammatory properties. Additionally, its potential benefits in addressing Alzheimer's disease, Parkinson's disease, multiple sclerosis, epilepsy, and cerebral injury are widely recognized¹⁰. In the context of inflammatory bowel disease (IBD), curcumin plays a regulatory role in maintaining the balance between oxidants and antioxidants. Furthermore, it influences the secretion of inflammatory mediators, such as TNF- α and nitric oxide¹¹.

Despite its therapeutic potential, curcumin exhibits several limitations, including low water solubility (approximately 0.4 mg/mL at pH 7.3), instability, and rapid decomposition at neutral and alkaline pH levels. Due to its hydrophobic nature, curcumin demonstrates low absorption, poor oral bioavailability, a high rate of intestinal metabolism, and rapid elimination from the body¹².

To achieve optimum therapeutic benefits, an adequate dose should be administered to inflamed tissues; therefore, a site-specific DDS is required. Moreover, low solubility is a challenge in DDS, which has led to the preparation of inclusion complexes of curcumin using cyclodextrin to improve the solubility, which may maximize the therapeutic efficacy, minimize dose, and help in drug loading into micro sponges, followed by presenting the drug in a micro spongy structure using pH-sensitive polymers to improve site-specific drug release. These microspongy polymeric structures using

pH-sensitive polymers can maximize anti-inflammatory therapy with a minimal drug dose and prolonged drug contact with inflamed tissues in the body.

MATERIAL AND METHODS

Materials

Curcumin was gifted by a cancer herbalist in Bangalore, India. Eudragit L100, S100 Degussa India Pvt. Ltd. and polyvinyl alcohol (PVA), and dibutyl phthalate from SD Fine Chemicals Ltd. All excipients were of pharmaceutical grade and the solvents were of analytical grade.

Preformulation studies

Compatibility study by Fourier Transform Infrared Spectroscopy (FTIR)

The FTIR spectra of curcumin and the physical mixture were recorded using Attenuated Total Reflection (ATR) (Bruker Alpha II). The sample was positioned on the holder, and IR spectra were obtained in the scanning range of 400-4000 cm^{-1} at a resolution of 1 cm^{-1} ¹³. The spectra was later generated for inclusion complex and also for the optimised formula.

Preparation of Curcumin Inclusion complexes

β -Cyclodextrin (β -CD) -drug inclusion complexes in the ratios listed in **Table 1** were prepared by the solvent evaporation method using a 1:1 ratio of methanol and acetone. β -CD was dissolved in China dish drug was added, and the solution was evaporated in an electric water bath with constant stirring till the solvent evaporated. Then, the product was scraped and passed through sieve No. 85 to get fine powder¹.

Table 1: Preparation of Curcumin β Cyclodextrin Inclusion complexes

SL.NO	Ratios	Drug (mg)	β - Cyclodextrin (mg)	Solvent	
				Methanol (ml)	Acetone (ml)
1	1:0.5	1000	500	10	10
2	1:1	1000	1000	10	10
3	1:1.5	1000	1500	10	10
4	1:2	1000	2000	10	10
5	1:2.5	1000	2500	10	10

Solubility Studies

Solubility analysis was performed for all ratios of curcumin-inclusion complexes. A calculated amount of curcumin inclusion complex was accurately weighed in a 10 ml volumetric flask containing phosphate buffer 7.4. The samples were maintained in a mechanical shaker for 48 h at 100 rpm. After 48 h, the solution was filtered, and the absorbance was determined using phosphate buffer 7.4 as a blank in a UV spectrophotometer at a wavelength of 418 nm¹³.

In vitro drug release

Drug release from the inclusion complexes was conducted using USP dissolution apparatus II at a stirring speed of 50 rpm at 37 ± 0.5 °C in 900 ml phosphate buffer (pH 7.4). Drug release was monitored for 3 h by collecting samples at 0.25, 0.5, 0.75, 1, 2, and 3 h. The drug concentration was determined against a phosphate buffer 7.4 as a blank in a UV spectrophotometer at 418 nm¹³.

Powder X-Ray diffraction (PXRD)

The XRD patterns of the pure drug and curcumin inclusion complexes were recorded at room temperature on a Bruker D8 Advance X-

ray diffractometer using Ni-filtered Cu K radiation (wavelength 1.540 Å). The data were recorded over a scanning range of 2 ° to 80°¹⁴.

Differential Scanning Calorimetry (DSC)

Five milligrams of the curcumin inclusion complex were precisely measured and placed in hermetically sealed aluminium pans, which were then crimped. The sample was heated from 0 °C to 200 °C at a rate of 10 °C/min. Throughout the measurement, a continuous purge of nitrogen at a flow rate of 40 mL/min was maintained, and DSC thermograms were recorded using a Shimadzu DSC-60 instrument.¹⁴.

Utilization of Custom experimental design

Based on preliminary trials, a custom design was used to optimize the formulation and processing parameters with the assistance of the design expert software version 13 on quality attributes such as % drug loading and % drug release. Formulation variables such as polymer concentration (mg) and PVA concentration (mg) were used as factors for the response of drug loading and drug release, as shown in **Table 2**¹⁵.

Table 2: Formulation table for the preparation of Microsponges.

Formulation code	Polymers conc. (mg)	PVA conc. (mg)	Inclusion complexes (mg) of (ratio 1:1.5)	Methanol (ml)	Distilled water (ml)
F1	200	455	250	20	20
F2	600	392	250	20	20
F3	204	326	250	20	20
F4	540	200	250	20	20
F5	600	392	250	20	20
F6	372	329	250	20	20
F7	372	329	250	20	20
F8	454	500	250	20	20
F9	200	200	250	20	20
F10	370	200	250	20	20
F11	372	329	250	20	20
F12	598	500	250	20	20

Formulations, F6, F7 and F11 are the three replicate points chosen to avoid the pure error and bias.

Preparation of microsponges

A polymer (1:1 Eudragit L100: Eudragit R100) solution was prepared in methanol using a magnetic stirrer. The drug was then dissolved in the above polymeric solution, 0.1 ml of dibutyl phthalate was added. Polyvinyl alcohol (PVA) in distilled water solution was added to the polymeric solution using a syringe (Gauge no. 5)) under constant stirring. After two h, the sample was allowed to settle and the precipitate obtained was filtered and washed several times with distilled water. The microsponges were dried overnight at room temperature and stored in a black closed container¹⁶.

Drug loading (%)

A calculated amount of the microsphere formulation was placed in Eppendorf tubes, and 2 ml of ethyl acetate was added to each tube. The tubes were vortexed for 5–10 min. The supernatant was diluted with methanol, and spectroscopic analysis was performed using methanol as a blank. From the above observations, the percentage drug loading was calculated by the below equation¹⁷.

$$\% \text{ Drug loading} = \frac{\text{Total drug} - \text{Free drug}}{\text{Total drug}} * 100$$

In vitro drug release

Initially, the drug release was studied in 0.1 N HCl to understand the integrity of the polymer in an acidic environment. A calculated amount of microsphere formulation was introduced into the USP dissolution test apparatus maintained at 50 rpm and 37 ± 0.5 °C, where 900 ml of 0.1 N HCl and phosphate buffer 7.4 were used as the dissolution medium, and the samples were withdrawn at 15, 30, 60, 120- and 180-min. Absorbance was determined using 0.1 N HCl/ phosphate buffer 7.4 as a blank in a UV method at 418 nm¹⁸.

Statistical analysis of In vitro drug release data

The data are presented as the mean \pm standard deviation (SD) of independent experiments. The in vitro drug release data were subjected to one-way Analysis of Variance (ANOVA) to determine the level of significance. Statistical significance was set at P value < 0.05 ¹⁹.

Selection of optimum formula and evaluation

From the experimental matrix, the design space and maximum desirability function helped reach the optimum formula.

Scanning electron Microscopy (SEM)

The sample was imaged using a scanning electron microscope (SEM) operated at an accelerating voltage of 10 kV with Hitachi SU 3500. A small quantity of the sample was affixed to a stub using a double-sided sticky carbon tape. The stub was then placed inside the SEM chamber under vacuum conditions and analysed at various magnifications, including 60X, 200X, 500X, 1,10 \times , and 2,50X, to achieve enhanced clarity in observing particle morphology/topology¹⁹.

Pharmacodynamic studies

Acetic acid-induced experimental Ulcerative Colitis in Colon: Wistar rats weighing 160–200 g (n=9) were approved by the Institutional Animal Ethical Committee (KCP/IAEC/PCOL/ PCEU /122/2023) and individually housed with unrestricted access to food and water.

The three groups(n=3) were: a) the negative controls (normal animals) received normal saline, b) positive control (colitis-induced, received 1 mL (4%) (v/v) of acetic acid through the intrarectal route), and c) treatment (colitis-induced and microsphere-treated orally in a 1% carboxymethyl cellulose dispersion at a calculated dose of 25 mg/kg, based on the human equivalent dose). After overnight fasting, mice were euthanized. Microsponges were administered every alternate day for one week. After one week, the animals were sacrificed, and the colon was isolated from all groups. Histopathological studies were performed by preserving the colon in a 10% formalin solution^{20,21}.

RESULTS AND DISCUSSION

Results

Preparation of Curcumin based β -Cyclodextrin Inclusion complexes

Curcumin inclusion complexes of cyclodextrin (1:0.5, 1:1, 1:1.5, 1:2, and 1:2.5) were prepared using a solvent evaporation method with a 1:1 ratio of methanol to acetone. The drug content of the ratios mentioned above was found to be 22.93 ± 0.25 , 39.09 ± 0.23 ,

55.47±0.54, 99.53±0.21, 78.80±0.4 and 61.90±0.16 %, respectively. β -CDs (referred to as host molecules) can form inclusion complexes with drugs (referred to as guest molecules) by taking part of a drug molecule into the central CD cavity. This changes the physicochemical properties of the drug. The formation of a drug/CD inclusion complex increases the aqueous solubility of the drug. An increase in solubility was observed when the concentration of the complexing agent was increased to 1.5 parts. However, solubility decreased thereafter. The formation of a drug-CD complex via a noncovalent bond, and in aqueous solution, the drug molecule within the complex and in solution remains in equilibrium. Drug molecules are readily released from complexes upon dilution with media or competitive complexation. However, the self-association of lipophilic molecules in aqueous media leads to reduced drug solubility at higher concentrations of complexing agents²². Solubility studies indicated that drug carrier 1:1.5 exhibited high solubility (99.53 ±0.21 µg/ml), as given in **Fig. 1**.

A study comparing the drug release of β -CD complexes with that of pure drugs revealed that the drug release rate increased at the ratios investigated. The highest drug release of 58.19±0.21% was observed at a 1:1.5 ratio after three h, due to the higher solubility of the drug in the solution. In the first 15 min, all the ratios showed a rapid initial drug release of 40%. This may be attributed to the initial drug wettability at the initial stages of the dissolution process and to the co-existence of the drug and β -CD in the dissolution medium or by the interaction between the hydrophilic outer surface and the drug²³. However, after 180 min, the 1:05, 1:1, and 1:1.5 ratios had drug release rates of 54.65±0.10, 53.23±0.32, and 58.19±0.21%, respectively. In contrast, the 1:2 and 1:2.5 ratios resulted in drug release rates of 49.54±0.13% and 48.54±0.53%, respectively. The lag phase may be due to the slow release of the drug from the interior of the cavity.²⁴ All four ratios showed a threefold increase in drug release compared to that of the pure drug, as depicted in **Fig. 2**.

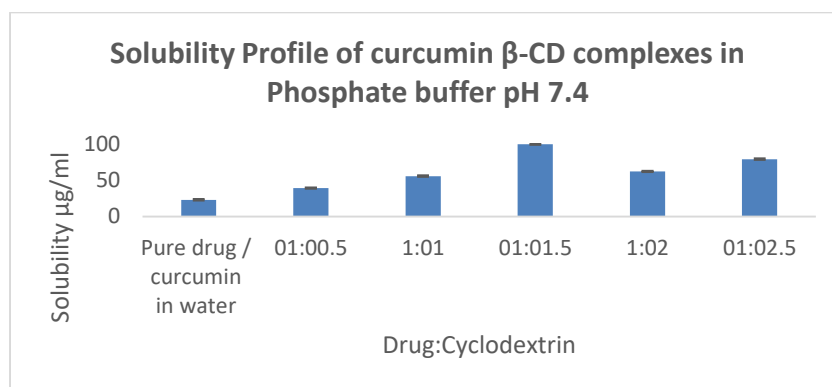


Fig. 1: Solubility profile of Curcumin- β -Cyclodextrin complexes in phosphate buffer pH 7.4.

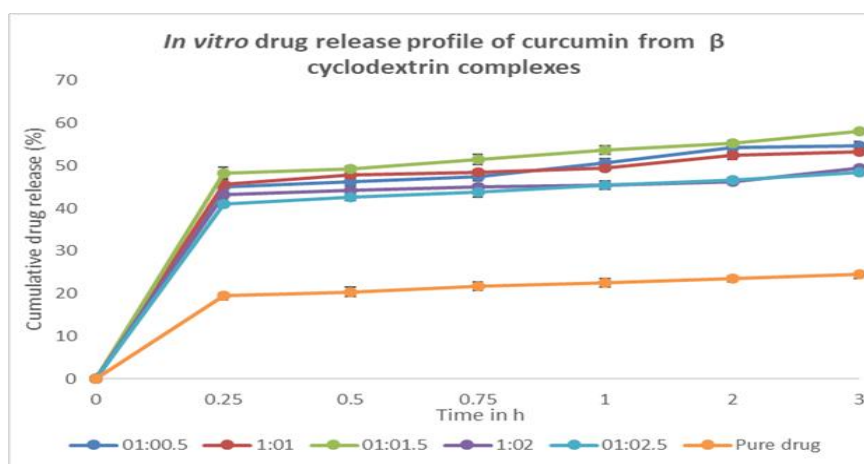


Fig. 2: *In vitro* drug release from Curcumin- β Cyclodextrin Inclusion complexes in Phosphate buffer pH 7.4.

PXRD

The X-ray diffraction (XRD) patterns of both the pure drug **Fig. 3 A** and the inclusion complexes of curcumin were collected within a scanning 2θ range of 2° – 80° . The X-ray pattern of the pure drug exhibited prominent peaks; however, in the complex, there was a reduction in the intensity and slight disorderly arrangement of peaks, as shown in **Fig. 3 B**, which shows the reduction in crystallinity and the contribution of cyclodextrin to improving the solubility.²³

Differential Scanning Calorimetry (DSC)

The thermal behavior of curcumin and its physical mixture was observed using DSC. The DSC thermogram of curcumin exhibited an endothermic peak at 182.22°C . The physical mixture exhibited a peak for the drug at 183.10°C and an endothermic peak at 316°C (reported value 300°C), which may be due to the melting point of cyclodextrin. DSC curves of the pure drug and the drug with excipients are shown in **Fig. 4**.

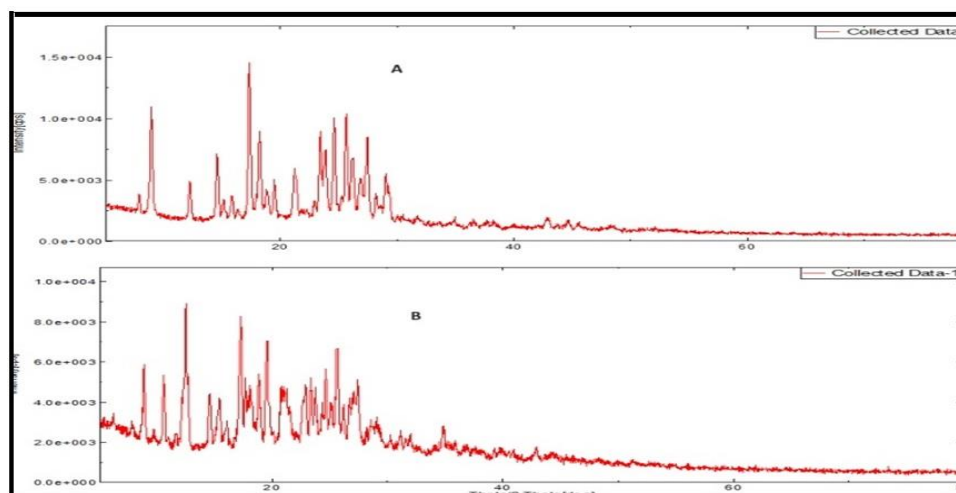


Fig. 3: X-Ray diffraction pattern of A) Curcumin, B) Curcumin -β Cyclodextrin inclusion complex.

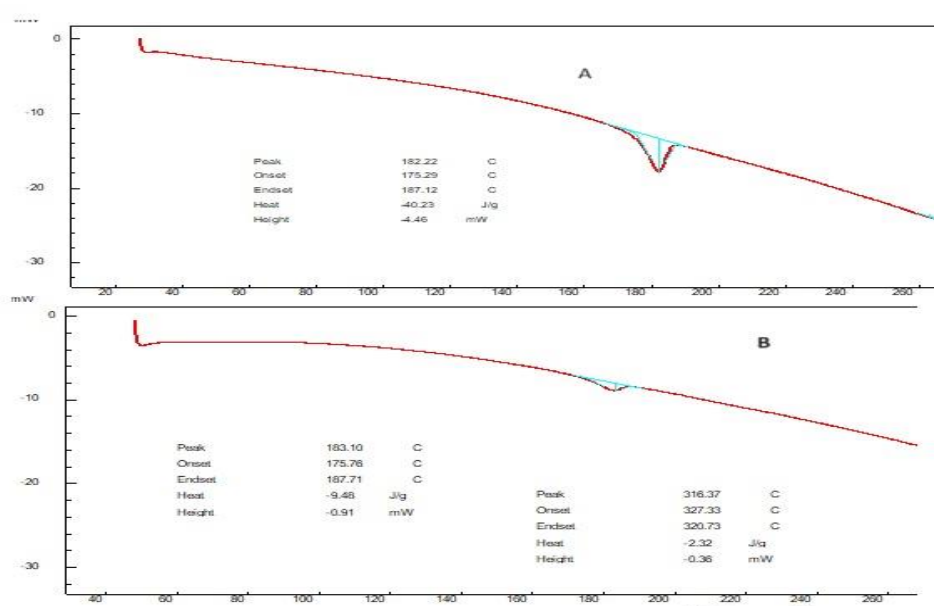


Fig. 4: DSC thermogram of A) Curcumin B) Physical mixture of curcumin and β Cyclodextrin inclusion complex.

Evaluation of Microsponges

Drug loading (%)

The drug loading of the prepared formulations ranged from 61.65 ± 0.74 % to 82.25 ± 0.34 %, as shown in **Fig. 5**. Both the polymer and PVA concentrations were found to influence drug loading. The polymer concentration alone did not influence drug loading. There was a remarkable contribution from PVA, as evident in the F3 formula with a maximum pay load of 82.25 ± 0.34 %, which may be the factor of an excess amount of surfactant in comparison to the polymer emulsifying the system properly avoiding the viscous forces, thus reducing the droplet size of the emulsion. The same theory may be explained for the drug loading of F5 with a vice versa effect.¹⁵

For F6, F7 and F11 which used the ratio of polymer to PVA is similar drug loading is observed. The large reservoir, explained by the optimum concentration of surfactant to the polymer resulted in it. The drug loading is also proposed to be factor of pore former used. They have the capacity to form minute pores which result in uptake of the dissolved drug into the system, later stage its solidification resulted in higher loading capacity¹⁶.

Drug release studies of the formulations under acidic conditions were negligible; therefore, they were not represented in the

present data. The results of the release profiles of microsponges in phosphate buffer (pH 7.4) are presented below: In 12 -h study, all 12 formulations exhibited > 90% with a maximum drug release of 97.34 ± 1.5 % (F3) and 90.11 ± 1.9 % (F5). Approximately 40% (**Fig. 6**) of the drug release was observed in the first 15 min for all formulations. This initial drug release may have contributed to the surface drug and initial swelling of the polymer, resulting in pore formation. During the next 3 h, 10 % drug diffusion occurred because of slow swelling of the polymer combinations at pH 7.4. However, controlled drug release was observed for all formulations for the next nine h and contributed to a maximum drug release of not less than 90%. The polymers Eudragit L100 and S100 were used in combination to achieve a pH-dependent drug release, in a sustained pattern to release the drug throughout the colon to accommodate the drug release during the colonic retention time of less than 13 h in general.¹⁷

The *in vitro* drug release data were subjected to one-way ANOVA analysis. A P value >0.05 indicates that there were no significant differences in the release profiles of the microsponges in the phosphate buffer at pH 7.4. Because there was no significant difference in the data, no further post hoc statistical analysis was performed. (**Table 3**).

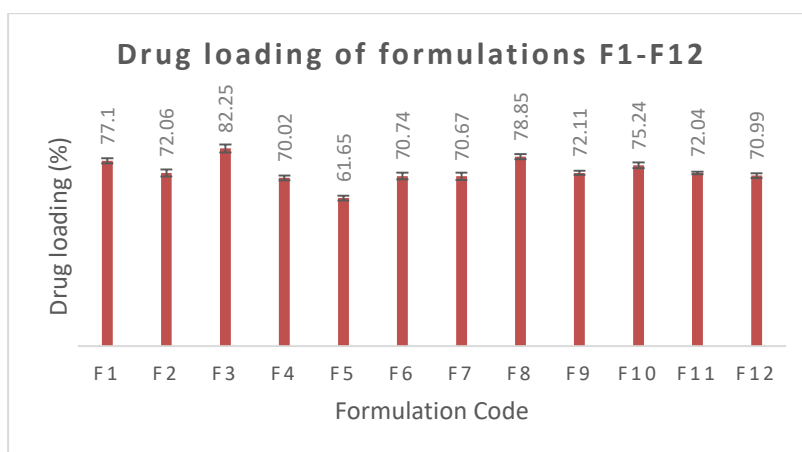


Fig. 5: Drug loading (%) of F1-F12 microsphere formulations.

Table 3: Statistical analysis of *in vitro* release data by ANOVA.

ANOVA						
Source of Variation	SS	df	MS	F	P-value	F crit
Between Groups	941.4192	11	85.58356	0.224567	0.995211	1.924308
Within Groups	27439.57	72	381.1052			
Total	28380.99	83				

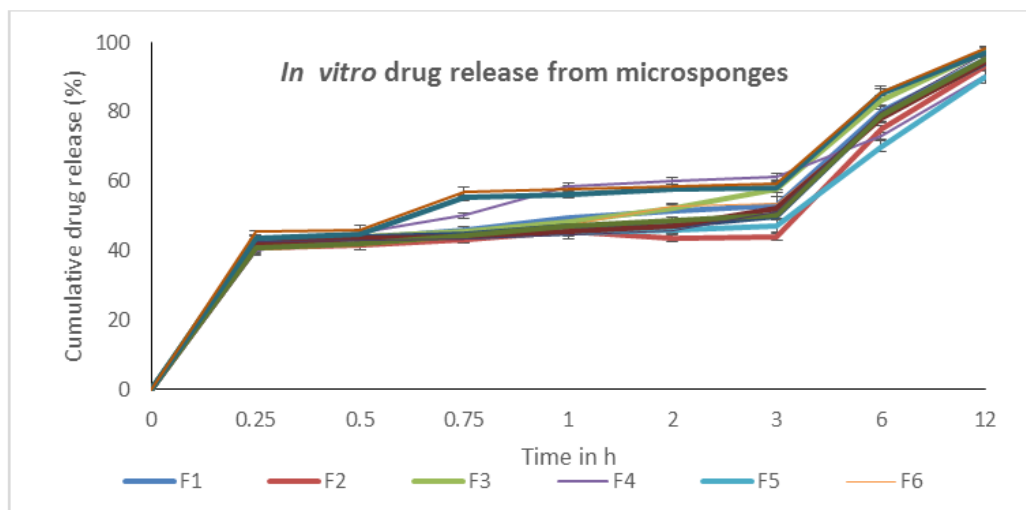


Fig. 6: *In vitro* drug release from F1-F12 microsp sponge formulations.

Evaluation of experimental design

Custom design is an experimental design that aims to enhance both the formulation and processing parameters of quality attributes, thereby leading to a designated design space. A summary of the model’s fit is presented in **Table 4**. The statistical significance of each factor, drug loading, and drug release in the selected data are given by P-values. P values of 0.0321 for drug loading and 0.0270 for drug release indicated that the chosen factors significantly affected the overall responses obtained. Drug loading had a linear relationship with polymer concentration; however, stabilizer concentration did not affect drug loading. Drug

release was significantly affected by PVA concentration, as mentioned earlier. The polynomial model equation (Equations 1 and 2) suggests a linear relationship between the factors chosen for the responses and absence of interactive effects. Desirability, an objective function, shows how closely the upper and lower limits are optimum²⁵. In the experimental design, at a maximum desirability of 1.00,25 the optimum formula was selected, as shown in **Fig., 7** and the numerical representation of the same is given in **Fig. 8**.

Drug loading = 67.68+4.95A+3.43B----(Eq-1)

Drug Release= 42.06+2.40A+3.79B ---(Eq -2)

Table 4: Statistical evaluation of model fit by ANOVA.

Source	Drug loading					Drug release %					Level of significance
	Sum of Squares	df	Mean Square	F-value	p-value	Sum of Squares	df	Mean Square	F-value	p-value	
Model	203.52	2	101.7	5.20	0.031	121.9	2	60.99	5.54	0.027	Significant
A-polymer conc	124.62	1	124.6	6.37	0.03	29.42	1	29.4	2.67	0.13	
B-PVA conc.	73.18	1	73.18	3.74	0.085	89.47	1	89.47	8.13	0.019	
Residual	176.14	9	19.57			99.03	9	11.00			
Lack of Fit	175.64	8	21.96	43.9	0.11	98.53	8	12.32	24.63	0.15	Not significant
Pure Error	0.5000	1	0.500			0.500	1	0.50			
Cor Total	379.67	11				221.0	11				

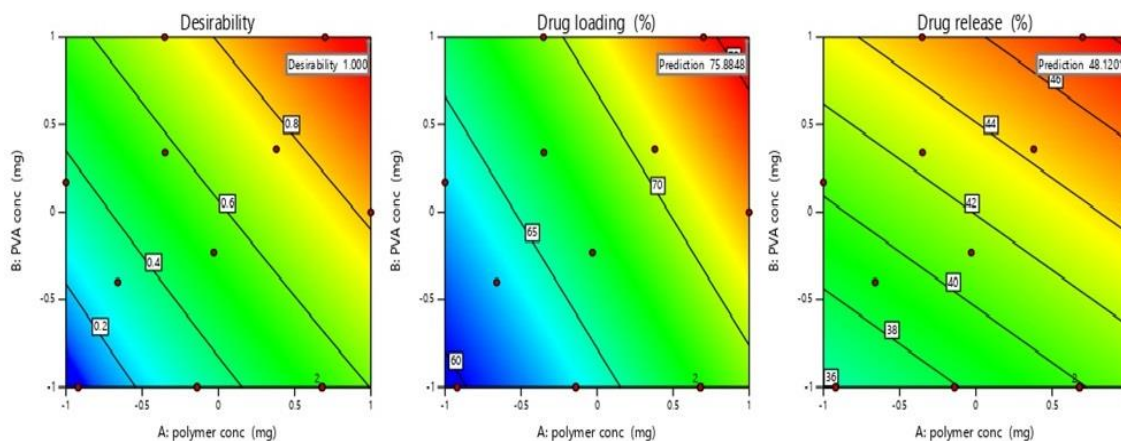


Fig. 7: Surface responses graph of drug loading and drug release at maximum desirability.

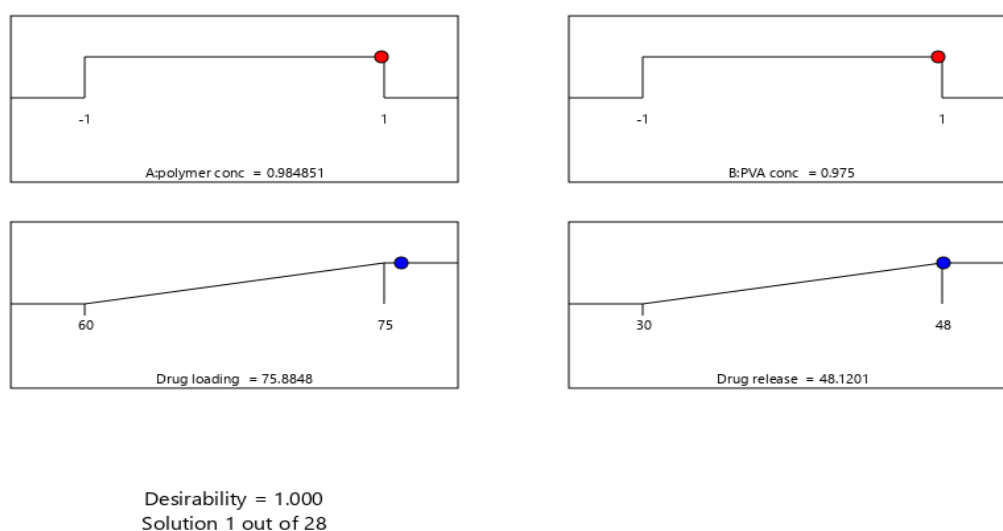


Fig. 8: Composition of optimum formula via numerical optimization at the maximum desirability.

Evaluation of optimized formula Comparative *in vitro* drug release studies

A comparative *in vitro* drug release study was carried out for a pure drug dispersion in comparison with the optimum microsphere formulation. The drug dispersion showed a release rate of $26.31 \pm 0.31\%$ in 3 h, whereas the optimum microspheres showed a release of 46.21 ± 0.23 at the end of first 3h. At the end of the 12 h study, 91.34% drug release was observed compared to 30% drug release from the dispersion. The greater drug release in comparison contributed to the reduced crystalline nature of the drug when presented in a β -cyclodextrin complexed form within

microspheres. The release of drug microspheres is a triphasic process, as the burst effect is seen in the initial hours, followed by slower drug release in the later 3 h, which may be due to drug diffusion via the pores, followed by subsequent lateral swelling of polymers along with added porosity and diffusion. contributed to a higher drug release pattern over the next six h, as shown in **Fig. 9**²⁶.

Surface morphology

The SEM images indicate fluffy structures and a disordered arrangement. The fluffy nature might have contributed to the pore forming agents used in the formula, depicted in **Fig. 10**.

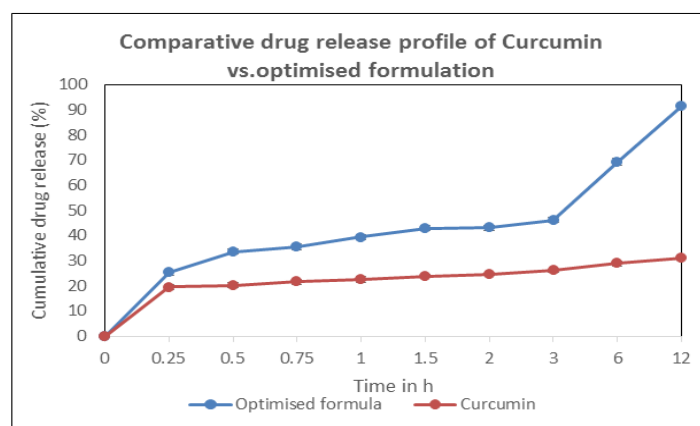


Fig. 9: Comparative *In vitro* drug release of optimize formula and pure drug in in Phosphate buffer pH 7.4.

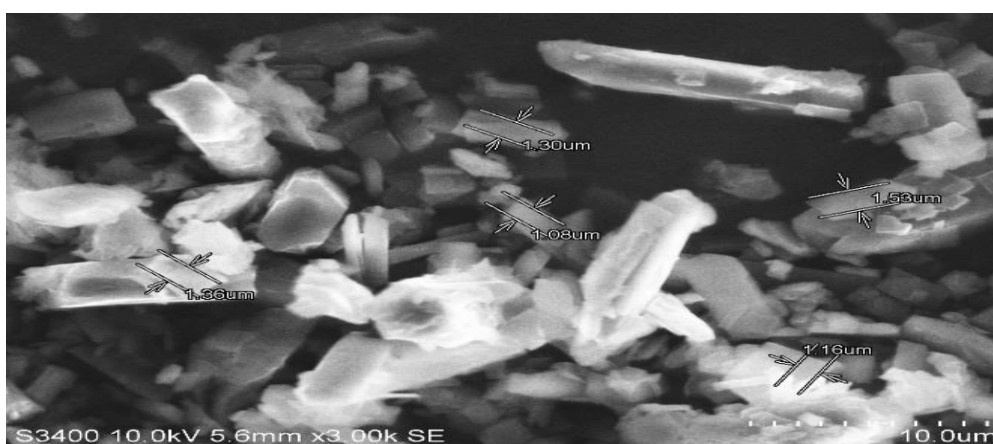


Fig. 10: Surface photograph of optimum microsponge formulation at 10 x magnification.

FTIR

Curcumin showed a characteristic peak at 3503.37 cm^{-1} due to phenolic OH stretching vibration; C=O stretching was observed at 1615.61 cm^{-1} and 1589.53 cm^{-1} . Also, C-O stretching at 1193.82 cm^{-1} , C=C stretching at 1498.19 cm^{-1} , and C-N at 1148.97 cm^{-1} appeared in the spectrum. All the above characteristic peaks appeared in the spectra of the pure drug and were also reflected in the physical mixture, inclusion complex, and optimized microsponge formula. The above observations suggest that there are no apparent incompatibility issues between the drug and additives¹⁴. However, a few additional peaks were observed in the physical mixture and due to excipients. (**Fig.11**). The overlay is shown in **Fig.12**.

Pharmacodynamic studies using ulcerative colitis model

Colitis observed in rat's manifests as crypt loss, infiltration of inflammatory cells in the mucosa and submucosa, submucosal oedema, erosion, and ulceration. Studies have demonstrated that exposure to 4% acetic acid for 15 s results in moderate superficial colitis on the first postoperative day. Acetic acid can disrupt the epithelial barrier and upset the balance between luminal antigens and intestinal immunity, thereby acting as the primary mechanism for colitis induction. Additionally, increased levels of reactive oxygen species (ROS) in inflammatory bowel disease (IBD) compromise the total antioxidant capacity (TAC) of intestinal cells. This in turn leads to a decline in the overall antioxidant system of intestinal cells, encompassing both enzymatic and non-enzymatic antioxidants. Histopathological evaluation in this study unveiled alterations in rat colon tissue

compared to normal mucosal cells, including negative changes in goblet cells and crypts (**Fig.13**) Meanwhile, rats treated with microsponges via the oral route retained well-compacted normal mucosal epithelium, crypts, and goblet cells with normal mucosal morphology. The findings from this study suggest that the test drug treatment could alleviate oxidative damage, such as ulceration,

congestion, goblet cell hyperplasia, mucosal damage with inflammation, and restoration of the colon histological architecture to normal²⁰. So, the pharmacodynamic study suggests the potential of healing the inflamed tissues and restoring the normal morphological and physiological condition, after administration of the microsponges.²¹

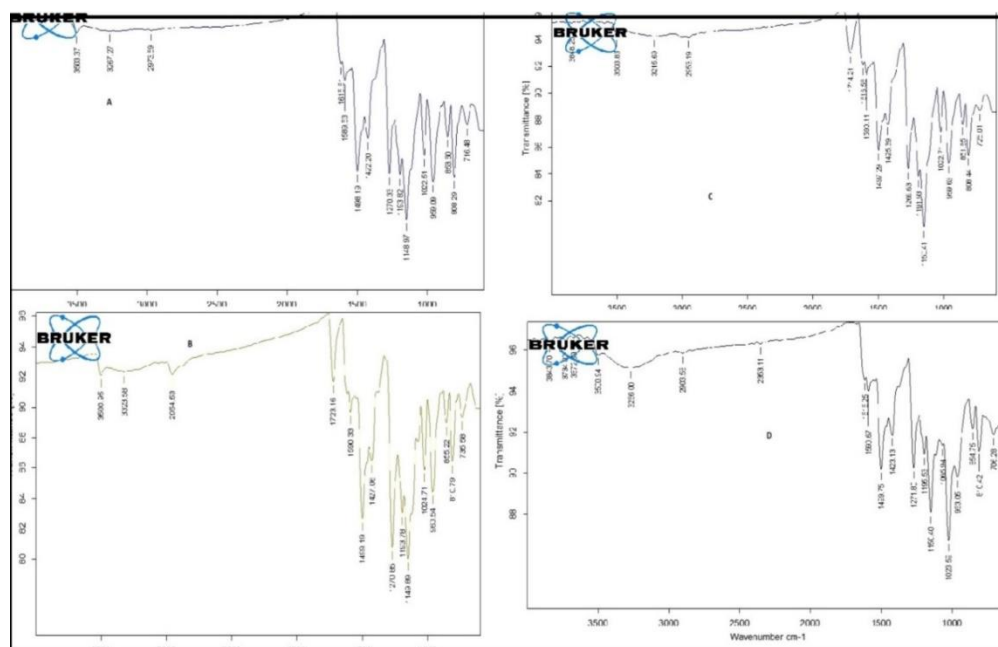


Fig. 11: FTIR spectra of A) curcumin B) Physical mixture of curcumin and β -cyclodextrin C) inclusion complex and D) Optimized formulation.

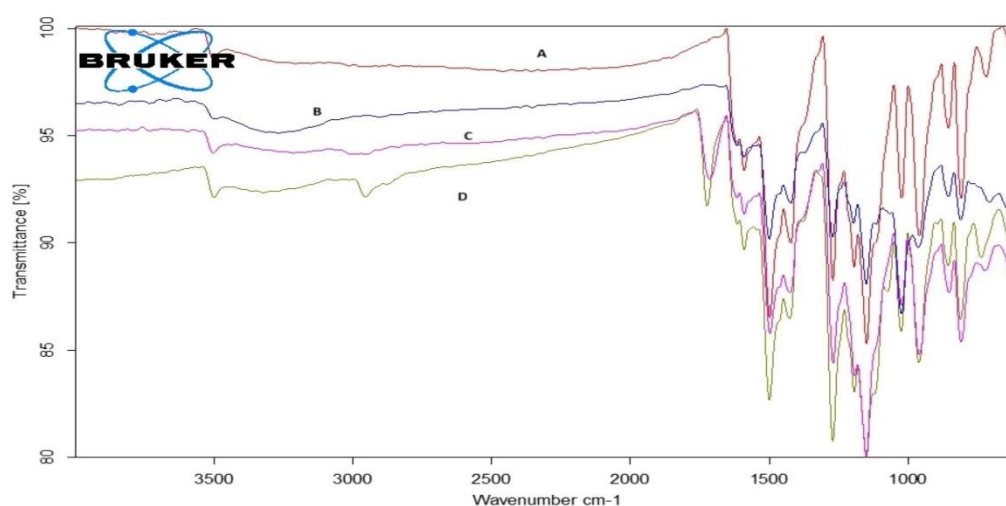


Fig. 12: Overlay IR spectra of A) curcumin B) Physical mixture of curcumin and β -cyclodextrin C) inclusion complex and D) Optimized formulation.

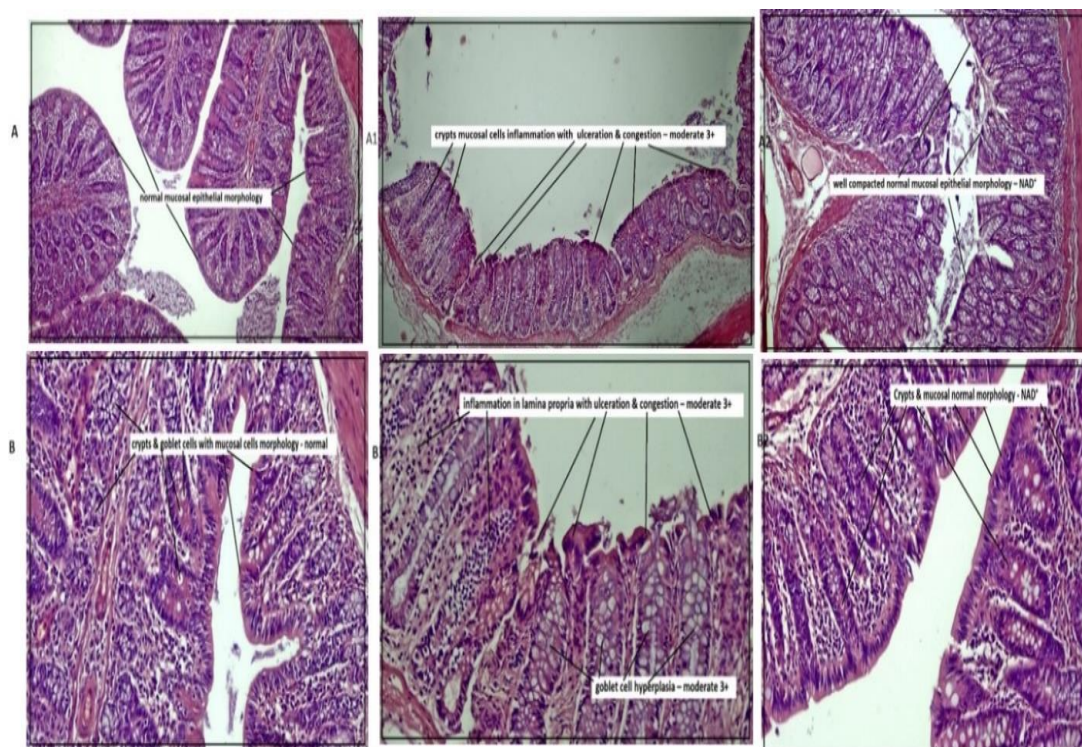


Fig. 13: Epithelial morphology (50X) of **A)** Negative control A1) positive control, A2) Treatment group. **B)** mucosal cells with goblet cells and crypts B1) crypts mucosal cells inflammation with ulceration and congestion – moderate 3+, B2) mucosal & goblet cell normal morphology.

Conclusion

In conclusion, microsponges, characterized by porous, polymeric bead-like structures featuring consistent voids and particle sizes ranging from 5-300µm, have proven to be efficient carriers for drug delivery. Employing a quasi-emulsion method with Eudragit L100 and PVA polymers successfully produced microsponges of curcumin, exhibiting a distinct microspungy structure. The inclusion complexes of curcumin within these microsponges significantly enhanced drug solubility by fourfold, enabling effective drug entrapment and promoting therapeutic action at lower doses. The custom design approach employed in this study facilitated the identification of the design space and the optimal formula using desirability analysis. Pharmacodynamic studies have demonstrated the potential of orally administered curcumin-loaded microsponges in alleviating inflammation-associated conditions in the colon. Consequently, the prepared microspunge formulation has emerged as a successful strategy for utilizing the natural anti-inflammatory agent curcumin for therapeutic applications.

REFERENCES

1. S. Amidon, J. E. Brown and V. S. Dave, "Colon-targeted oral drug delivery systems: Design trends and approaches", *AAPS PharmSciTech*, 16(4), 731–741 (2015).
2. G. Lemmens, A. Van Camp, S. Kourula, T. Vanuytsel and P. Augustijns, "Drug disposition in the lower gastrointestinal tract: Targeting and monitoring", *Pharmaceutics*, 13(2), 161 (2021).
3. M. K. Sarangi, M. E. B. Rao and V. Parcha, "Smart polymers for colon targeted drug delivery systems: a review", *Int J Polym Mater*, 70(16), 1130–1166 (2021).
4. Y. Ren, L. Jiang, S. Yang, *et al.*, "Design and preparation of a novel colon-targeted tablet of hydrocortisone", *Braz J Pharm Sci*, 53(1), e15009 (2017).
5. M. M. Patel, T. J. Shah, A. F. Amin and N. N. Shah, "Design, development and optimization of a novel time and pH-dependent colon targeted drug

- delivery system", *Pharm Dev echnol*, 14(1), 65–72 (2009).
6. S. Sudarshan, S. Sangeetha, N. R. Sheth, P. Roshan, Y Ushir and R. Gendle, "Colon specific drug delivery system of mesalamine for eradication of ulcerative colitis", *Res J Pharm Tech*, 2(4), 819–823 (2009).
 7. S. C. Fassihi, R. Talukder and R. Fassihi, "Colon-targeted delivery systems for therapeutic applications: Drug release from multiparticulate, monolithic matrix, and capsule-filled delivery systems", in ACS Symposium Series, Washington, DC: American Chemical Society, 309–338 (2019).
 8. P. D. Borawake, A. Kauslya, J. V. Shinde and R. S. Chavan, "Microsponge as an emerging technique in novel drug delivery system", *J Drug Deliv Ther*, 1(1), 171–182 (2021).
 9. S. Rajeswari and V. Swapna, "Microsponges as a neoteric cornucopia for drug delivery systems", *Int J Curr Pharm Res*, 11(3), 4–12(2019).
 10. P. Arya and K. Pathak, "Assessing the viability of microsponges as gastro retentive drug delivery system of curcumin: Optimization and pharmacokinetics", *Int J Pharm*, 460(1–2), 1–12 (2014).
 11. K.K. Majumder, J. B. Sharma, M. Kumar, *et al.*, "Development and validation of UV-Visible spectrophotometric method for the estimation of curcumin in bulk and pharmaceutical formulation", *Pharmacophores*, 10(1), 115–121 (2020).
 12. S.K. Savale, "Curcumin as a model drug: conformation, solubility estimation, morphological, in vitro, and in vivo biodistribution study", *J Pharm Sci Tech*, 7(1), 31–35 (2017).
 13. C. S. Mangolim, C. Moriwaki, A. C. Nogueira, *et al.*, "Curcumin- β -cyclodextrin inclusion complex: Stability, solubility, characterisation by FT-IR, FT-Raman, X-ray diffraction and photoacoustic spectroscopy, and food application", *Food Chem*, 153, 361–370 (2014).
 14. P. R. K. Mohan, G. Sreelakshmi, C. V. Muraleedharan and R. Joseph, "Water soluble complexes of curcumin with cyclodextrins: Characterization by FT-Raman spectroscopy", *Vib Spectrosc*, 62, 77–84 (2012).
 15. D. Hales, L. Ruxandra Tefas, I. Tomuță, *et al.*, "Development of a curcumin-loaded polymeric microparticulate oral drug delivery system for colon targeting by quality-by-design approach", *Pharmaceutics*, 12(11), 1027 (2020).
 16. R. Sareen, K. Nath, N. Jain, and K. L. Dhar, "Curcumin loaded microsponges for colon targeting in inflammatory bowel disease: Fabrication, optimization, and *in vitro* and pharmacodynamic evaluation", *Biomed Res. Int*, 2014,340701, 1–7 (2014).
 17. S. Janakidevi and K. V. Ramanamurthy, "Development of colon-targeted microsponges for the treatment of inflammatory bowel disease", *Indian J Pharm Sci*, 80(4), 604–60 (2018).
 18. D. Guzman-Villanueva, I. M. El-Sherbiny, D. Herrera-Ruiz and H. D. C. Smyth, "Design and *in vitro* evaluation of a new nano-microparticulate system for enhanced aqueous-phase solubility of curcumin", *Biomed Res Int*, 2013, 1–9 (2013).
 19. R. Deshmukh, R. K. Harwansh, S. D. Paul and R. Shukla, "Controlled release of sulfasalazine loaded amidated pectin microparticles through Eudragit S 100 coated capsule for management of inflammatory bowel disease", *J Drug Deliv Sci Technol*, 55, 101495 (2020).
 20. G. Owusu, D. D. Obiri, G. K. Ainooson, *et al.*, "Acetic acid-induced ulcerative colitis in Sprague Dawley rats is suppressed by hydroethanolic extract of *Cordia vignei* leaves through reduced serum levels of TNF- α and IL-6", *Int J Chronic Dis*, 2020, 1–11 (2020).
 21. E. A. Adakudugu, E. O. Ameyaw, E. Obese, *et al.*, "Protective effect of

- bergapten in acetic acid-induced colitis in rats", *Heliyon*, 6(8), e04710 (2020).
22. S. Guo, "Encapsulation of curcumin into β -cyclodextrins inclusion: A review", *E3S Web Conf*, 131, 01100 (2019).
 23. D. Sid, M. Baitiche, Z. Elbahri *et al.*, "Solubility enhancement of mefenamic acid by inclusion complex with β -cyclodextrin: *in silico* modelling, formulation, characterisation, and *in vitro* studies", *J Enzyme Inhib Med Chem*, 36(1), 605–617 (2021).
 24. P. Saokham, C. Muankaew, P. Jansook and T. Loftsson, "Solubility of cyclodextrins and drug/cyclodextrin complexes", *Molecules*, 23(5), 1161 (2018).
 25. Ashwini, P. Sudheer, B. S. Sogali, and Chandramouli, "Development optimization and cytotoxicity evaluation of glyburide loaded nanostructured lipid carriers", *Ind J Pharm Educ*, 56(2s), 189–199 (2022).
 26. P. Pawar, R. Mehta, A. Chawla and P. Sharma, "Formulation and *in vitro* evaluation of Eudragit S-100 coated naproxen matrix tablets for colon-targeted drug delivery system", *J Adv Pharm TechnolRes.*, 4(1), 31-41 (2013).



نشرة العلوم الصيدلانية جامعة أسيوط



تطوير وتقييم الإسفنج الايدراجيت الدقيق لقرار الكركمين كعلاج مضاد لالتهابات القولون

سيد محسن عباس - بريثي سودهير *

قسم الصيدلانيات، كلية كروباندي للصيدلة، بنغالورو ٥٦٠٠٣٥، الهند

تهدف هذه الدراسة إلى تطوير الإسفنج الدقيق الكركمين لمكافحة التهاب القولون. تم التعرف على الكركمين تقليدياً لخصائصه المضادة للالتهابات. ومع ذلك ، فإن إمكاناتها العلاجية تعوقها عوامل ، مثل التوافر البيولوجي المنخفض ، وضعف الذوبان في الماء ، وعدم الاستقرار في البيئات الحمضية والمحايدة. بالإضافة إلى ذلك ، فإن امتصاصه المحدود من الأمعاء ، والتمثيل الغذائي الكبدي ، والتخلص السريع يحد من فعاليته. لمعالجة هذه المشاكل ، تهدف هذه الدراسة إلى تحسين قابلية ذوبان الكركمين عن طريق إنشاء متراكبات تضمين باستخدام السيلولوديكسترين. يمكن لهذه المتراكبات تعزيز الفعالية العلاجية ، وتقليل الجرعة المطلوبة ، وتسهيل تحميل الدواء في الإسفنج الدقيق. بدأت هذه الدراسة بإنشاء متراكبات إدراج الكركمين مع السيلولوديكسترين ، والتي تم تقييمها لمحتواها من العقار ، والذوبان ، والإنطلاق في المختبر ، والخصائص التركيبية. بالإضافة إلى ذلك ، تم تطوير الإسفنج الدقيق من سيلولوديكسترين باستخدام بوليمرات حساسة لدرجة الحموضة (ايدراجيت L100 و ايدراجيت S 100) ومكون للمسام (PVA) ، استرشادا بالتصميم التجريبي (Design Expert الإصدار ١٣) لتحسين تحميل العقار و انطلاقه. خضعت المتراكبات الناتجة لتقييمات FTIR و SEM والنشاط المضاد للالتهابات باستخدام نموذج التهاب القولون الناجم عن حمض الخليك. أظهرت متراكبات التضمين بنسبة ١:٥ ، ١:١٠ ، و ١:٢٠ خصائص مرغوبة ، وأظهر الإسفنج الدقيق الأمثل زيادة بمقدار ثلاثة أضعاف في معدل إطلاق العقار مقارنة بالعقار منفرداً. يشير التأثير المضاد للالتهابات الذي لوحظ في القولون ، كما يتضح من استعادة التشكل الطبيعي بعد تناوله عن طريق الفم للإسفنج الدقيق ، إلى إمكانات التركيبة المثلى لتوصيل الدواء المستهدف. في الختام ، أظهرت الإسفنج الكركمين الذي تم تطويره باستخدام الايدراجيت تأثيرات مضادة للالتهابات على أنسجة القولون.